



Test of a novel 2×2 multi-anode MCP-PMT

Ziwei Li^{1,3} · Xin Li^{1,3} · Ping Chen² · Cheng Li^{1,3} · Yonglin Wei² · Xiaofeng Sai² · Jianbei Liu^{1,3} · Ming Shao^{1,3} · Jinshou Tian² · Hulin Liu²

Received: 26 May 2020 / Revised: 7 August 2020 / Accepted: 26 August 2020 / Published online: 18 September 2020
© Institute of High Energy Physics, Chinese Academy of Sciences 2020

Abstract

Purpose Xi'an Institute of Optics and Precision Mechanics of CAS is developing a novel MCP-PMT with 2×2 matrix anode pixels with a time resolution of picosecond level. It is composed of a cermet shell, bi-alkali photocathode, and V-type cascade MCP layers. In order to study the method of measuring the characteristics of such MCP-PMT with picosecond time resolution, we develop a PMT test system to test its performance.

Methods A voltage divider resistor circuit for the MCP-PMT is designed to meet the requirements of both high gain and fast time response. The test system includes a picosecond laser source in the single-photon mode, a high-bandwidth oscilloscope, and another fast MCP-PMT as reference. Full waveforms of PMT signals are collected and analyzed offline. The overall system time error is 26 ps.

Results The test result shows that the gain of the MCP-PMT achieves 1×10^7 . The transit time spread (TTS) of all channels is better than 60 ps (σ). The uniformity and crosstalk among adjacent channels are also studied by scanning each channel's response along the photocathode plane.

Conclusions The MCP-PMT shows excellent timing performance and the potential of achieving better spatial resolution by further pixelation.

Keywords MCP-PMT · Picosecond timing · Performance test · Cherenkov detection

Introduction

In the experimental nuclear and particle physics, due to the high energy and luminosity of new-generation particle accelerators, the variety and phase space range of the final state particles produced by collisions greatly increase. Therefore, the identification of high-density, high-momentum (up to several GeV) particles becomes a key issue and required the particle identification (PID) detector and its photosensitive PMT units to achieve the high time resolution up to picosecond level [1, 2]. For example, the high luminosity upgrade of the Large Hadron Collider (HL-LHC) at CERN aims at the

high luminosity of $5 \times 10^{34}/\text{cm}^2 \text{ s}$ @ 14 TeV, which will double the number of hit particles per unit area of the detector. The radiation dose will reach $5 \times 10^6 \text{ Gy}$ @ $R = 5 \text{ cm}$, more than 100 times the current level [3, 4]. The tracks' high density and pileup effect, as well as the background radiation, will greatly deteriorate the track reconstruction efficiency, causing the uncertainty of the secondary decay vertex and a large number of tracking loss for neutral particles, and reducing the measurement accuracy of the detector. According to the simulation and experimental data, it is expected that if the detector's time resolution reaches 30 ps @ 30 GeV photons, the pileup effect can be reduced by more than 10 times [5].

To meet this requirement, the Cherenkov detector has become an ideal option because of its fast time response, high radiation resistance and wide applicability. One important feature of the Cherenkov radiation generated is directly related to the kinematic parameters (velocity β) and almost immediately when the relativistic charged particles pass through Cherenkov radiator. The duration of the light pulse is determined by the characteristics of the radiator material and the photosensitive device. For example, the intrinsic pulse

✉ Xin Li
li124ste@ustc.edu.cn

¹ State Key Laboratory of Particle Detection and Electronics, University of Science and Technology of China, Hefei 230026, China

² Xi'an Institute of Optics and Precision Mechanics, CAS, Xi'an, China

³ Department of Modern Physics, University of Science and Technology of China, Hefei 230026, China

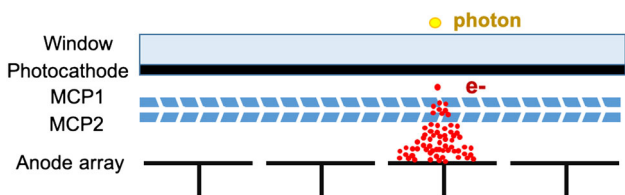


Fig. 1 The schematic of MCP-PMT

duration of high-purity fused quartz (1 cm thick) is about 10^{-11} s, which is 2–3 orders of magnitude faster than ordinary organic scintillation, with small statistical fluctuation. Because the wavelength of Cherenkov radiation is mainly within the ultraviolet (UV) range and the number of photons radiated per unit path length is small, the performance of the Cherenkov detector mainly depends on the time characteristics and spectral response of the photosensitive sensor. Therefore, the UV-sensitive microchannel plate PMT (MCP-PMT) is the preferred photoelectric converter for Cherenkov light detection [6, 7].

In this paper, we introduce the methods to measure the characteristics of MCP-PMT with picosecond time resolution, including the gain, single photoelectron spectrum, transit time spread (TTS) and the uniformity and crosstalk between anode pads. The MCP-PMT prototype we tested is developed by Xi'an Institute of Optics and Precision Mechanics of CAS.

Structure and signal of the MCP-PMT

Structure

Microchannel plate is a special electron multiplier with a fast time response, good spatial resolution, high gain and low noise. It multiplies the electrons collected in the inner microchannel by the secondary electron emission, amplifying the electron current by more than ten thousand times. The MCP-PMT is consisted of an acceptance window, photocathode deposited inside the window, two-stage MCP and multi-channel readout anode, as shown in Fig. 1, when the photons are incident into the acceptance window and converted into photoelectrons in the photocathode by the photoelectric effect. Photoelectrons are accelerated under the electric field between the photocathode and MCP1, transit to MCP1, and multiplied by 10^3-10^4 times. Then the photoelectrons continue the transition from MCP1 to MCP2 and are multiplied again, with the total gain of 10^6-10^8 . Finally, each measurable single photoelectron from MCP2 is collected by the multi-channel anode and output signal.

The MCP-PMT sample we tested is a 2×2 matrix anode MCP-PMT, composed of a cermet shell, bi-alkali photocathode, V-type cascade MCP layers with characteristics of high

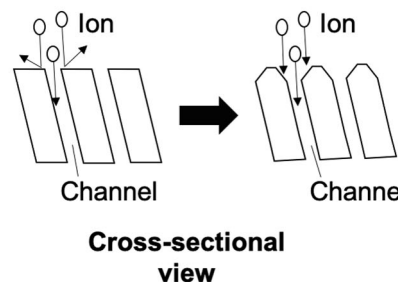
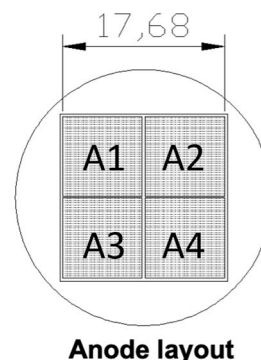
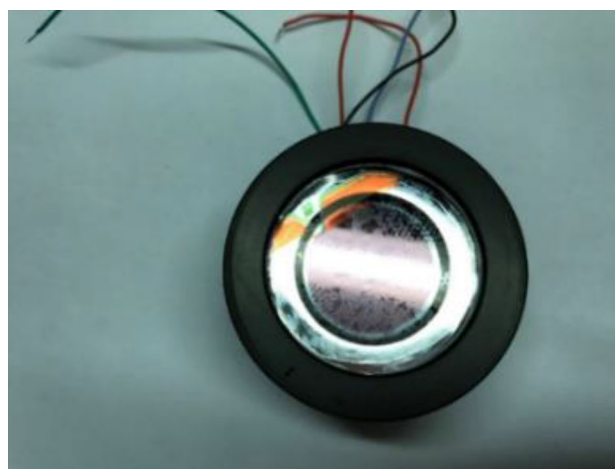


Fig. 2 Photo of the multi-anode MCP-PMT prototype (left); the drawing of the size of its anode and the cross-sectional view of V-type cascade MCP (right)

gain around 10^7 and UV sensitivity in the wavelength around 300 nm. Each pixel size is $9 \text{ mm} \times 9 \text{ mm}$, as shown in Fig. 2. The MCP surface is coated with high SEY (secondary electron yield) material to increase its collection efficiency. To optimize the timing performance up to the picosecond level, it applies the proximity MCP structure with a strong electric field: the spacing between the photocathode and the MCP1, as well as the spacing between MCP2 output and the anode, is less than 2 mm, which greatly reduces the electron's flight time and improves the timing accuracy. The pore diameter of the MCP is $10 \mu\text{m}$, and the bias angle is less than 12° .

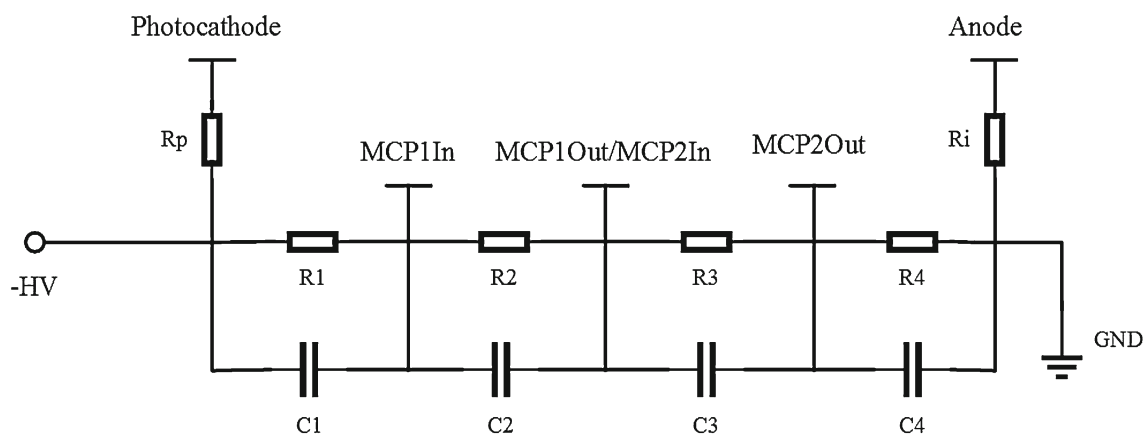


Fig. 3 Voltage divider circuit

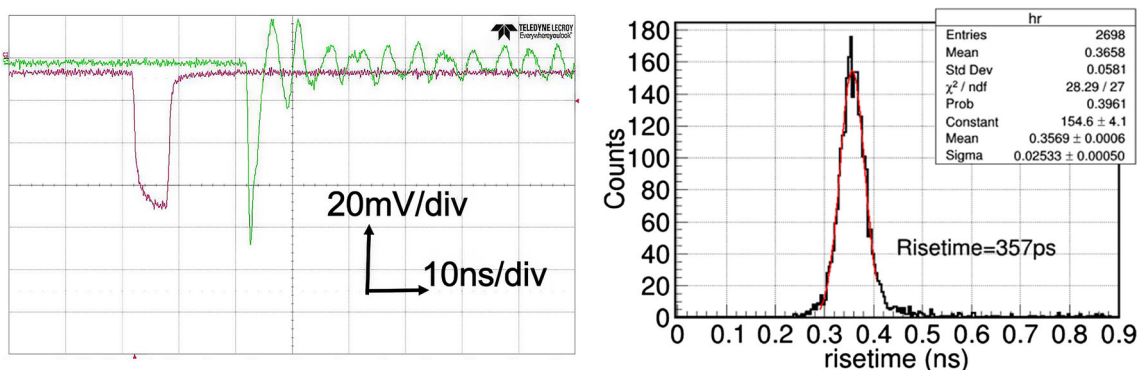


Fig. 4 Typical output pulse of MCP-PMT measured in the single-photon (HV = 2200 V). The red line represents the trigger signal

Output signal

A voltage divider resistor circuit for the MCP-PMT is designed as shown in Fig. 3. The voltage ratio is 3:7:7:2 (Photocathode-MCP1In-MCP1out/MCP2In-MCP2Out-Anode) to meet the requirements of both high gain and fast time response. Figure 4 shows that the output pulse under the single-photon intensity at voltage 2200 V read out by a 50 Ω SMA cable connected to a digital high bandwidth oscilloscope (LeCroy WM813ZI-A), it exhibits a sharp shape with a “ringing” tail (will be discussed in “Characteristics measurement of MCP-PMT” section). The average rise time of signals is 357 ps, and the pulse duration is around 2 ns.

Test setup

The experimental setup is shown in Fig. 5. The picosecond laser source (HAMAMATSU PLP10-038) provides a light pulse with a wavelength of 375 nm and a width of 49 ps.

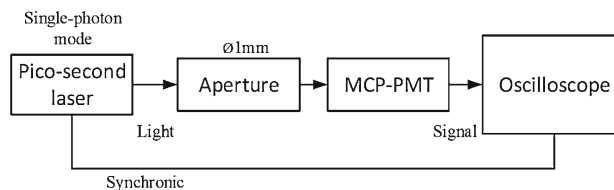


Fig. 5 Schematic diagram of the test setup

It is tuned in the single-photon mode guided by an optical fiber through an attenuator and an aperture of 1 mm diameter. The anode output of the MCP-PMT is directly fed into a high bandwidth oscilloscope (LeCroy WM813ZI-A). Meanwhile, the laser also provides a synchronic signal as the trigger and time reference to the oscilloscope. Full waveforms of signals are collected and analyzed offline. The synchronic signal is calibrated by a fast MCP-PMT (R3809, TTS = 20 ps), and the statistical errors of time fluctuations $\sigma_{\text{SYC}} \sim 14$ ps are shown in Fig. 6. Overall, the system time error is estimated as: $\sigma_{\text{system}} = \sqrt{\sigma_{\text{SYC}}^2 + \sigma_{\text{ps Laser}}^2} \sim 26$ ps.

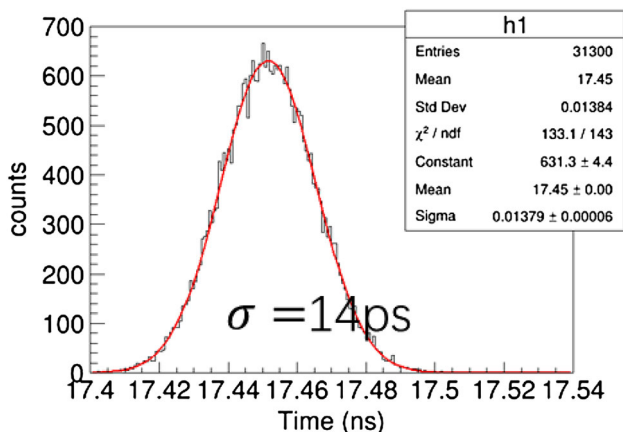


Fig. 6 Time fluctuations of synchronic signal calibrated

Characteristics measurement of MCP-PMT

Gain

At the high voltage (HV) of 1900 V, the charge distribution of single photoelectron (SPE) is measured as shown in Fig. 7a. Because the single can induce some double or triple photoelectrons except for obvious SPE, a combined fit is applied (as shown in formula 1) to estimate the contribution of first, second and third photoelectron.

$$f(x) = \sum_{i=0}^n P_i(\lambda) \times \frac{1}{\sqrt{2\pi}\sigma_i} e^{-\frac{(x-\mu_i)^2}{2\sigma_i^2}} \quad (1)$$

where $P(\lambda)$ is Poisson distribution and λ is the mean number of induced photoelectrons in expectation, σ and μ are Gaussian parameters to fit the contribution of each photoelectron. The i represents first, second and third photoelectron, and $i = 0$ is the pedestal background. According to the fitting parameters, the anode gain is 1.29×10^7 calculated by the formula (2).

$$\text{Gain} = \frac{\mu_{PE1} - \mu_{ped}}{e} \quad (2)$$

Here, μ_{PE1} is the peak charge of the first photoelectron, μ_{ped} is the peak charge of the pedestaled by noise, and e is the single-electron charge of $1.6 \times 10^{-19}C$.

TTS

Figure 7b shows the TTS measurement of the anode. It is estimated as the leading edge time difference between the MCP-PMT signal and the synchronic signal. To avoid the time walk, we use 20% amplitude fraction as the leading edge time threshold. Due to electrons recoiling from the MCP surface, a tail within a small time interval is observed in

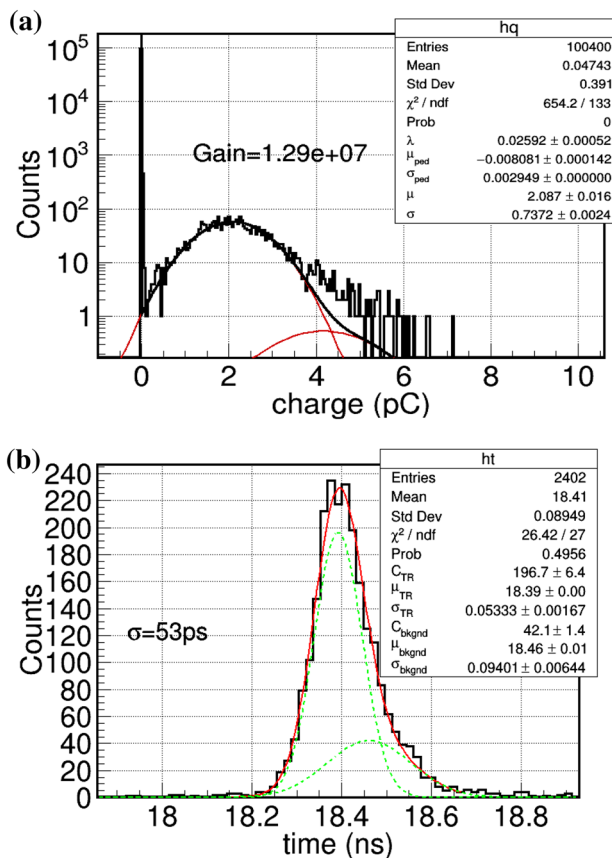


Fig. 7 Measured characteristics of the MCP-PMT: **a** single photoelectron spectrum, **b** time transit spread (TTS)

the TTS distributions. This distribution is fitted by a double-Gaussian function $g(x)$, as shown in formula 3.

$$g(x) = \frac{1}{\sqrt{2\pi}\sigma_S} e^{-\frac{(x-\mu_S)^2}{2\sigma_S^2}} + \frac{1}{\sqrt{2\pi}\sigma_{re}} e^{-\frac{(x-\mu_{re})^2}{2\sigma_{re}^2}} \quad (3)$$

where σ_S and μ_S are standard deviation and mean from the true signal, as well as σ_{re} and μ_{re} are standard deviation and mean from recoiled electrons. The TTS is estimated as 53 ps corresponded to the standard deviation of the narrow peak.

Uniformity

The MCP-PMT's uniformity is measured by a one-dimension scan across the active area of the anode. The laser source is tuned in the single-photon mode through an aperture of 1 mm diameter, making scan points with ~1 mm diameter on the PMT. The positions of 7 scan points are shown in Fig. 8. All scan points are located in the sensitive area of the anode A1. The scanning direction along the diagonal line of A1 to A4 is from outside to inside. All measurements are readout from A1 anode. The performance of the MCP-PMT (TTS and gain) in Fig. 9 shows obvious degradation

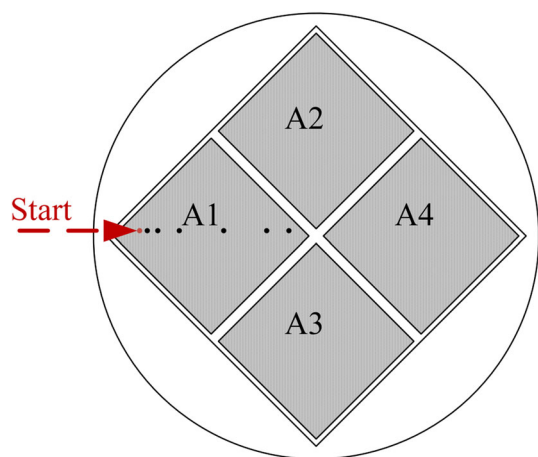


Fig. 8 The 1-d scan of uniformity

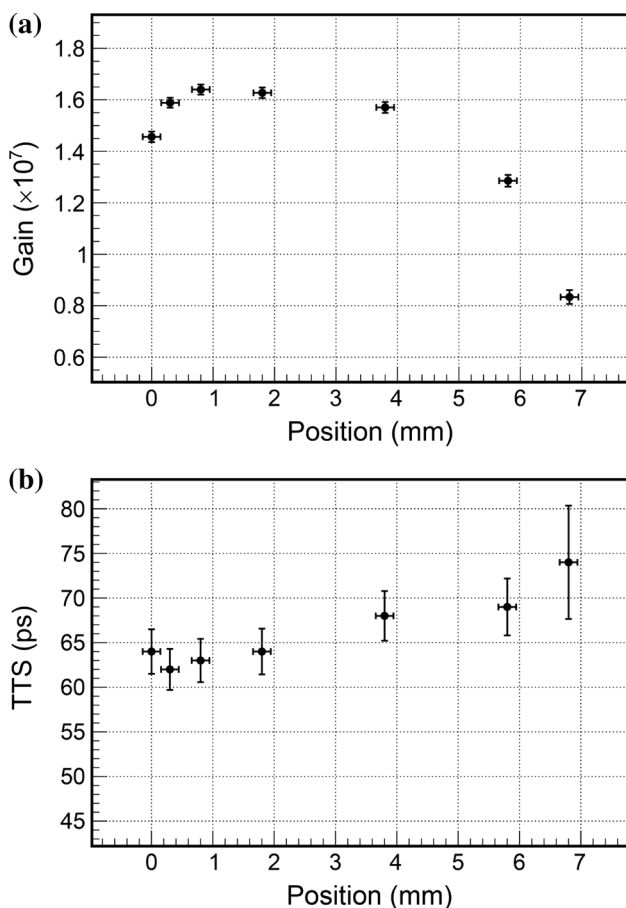


Fig. 9 The discordance of TTS is observed in the scanning at local: **a** gain as a function of scanned position, **b** TTS as a function of scanned position

as the scan point moves closer to the PMT center. It might be because of the PMT's dead area: the cascaded electron cloud induced in the MCP is much larger than the scan point itself (as shown in Fig. 1). The size of the electron cloud mainly depends on the distance and electric field between the

photocathode and the anode. Therefore, when the scan point moves closer to the dead area, more cascaded electrons will enter the dead area and be lost, making a larger fluctuation in transit time. Besides, it is easier for electrons to escape to neighbor pixels when the scan points closer to the PMT center. The decrease in the numbers of electrons results in the drop of gain. And the charge-sharing signal of neighbor pixels could induce crosstalk overlapping in the true signal of A1, reducing the height of the true signal and deteriorating its time performance. Similarly, the divergence of the first scan point is due to its location near the pad edge which is closer to the dead area. For more detailed study on the uniformity, delicate scanning of the entire sensitive area remains further test.

Signal crosstalk

As Fig. 10 shows, when one channel of the MCP-PMT (A1) with a 1 mm diameter aperture is illuminated by the single photon, the crosstalk in other channels (A2, A3, A4) is observed. The shape and amplitude of each crosstalk are similar and independent on the distance of anode from the illuminated one. The first induced amplitude of crosstalk is inverted and about 1/6 of the signal. Besides, all channels have tails as decaying sine (ringing). To prevent "ringing", the voltage divider circuit needs to be improved in the next.

As Fig. 11 shows, the crosstalk might be induced through the last electrode, facing the anodes of the second MCP layer. The anode and the last electrode of the MCP, separated by a vacuum gap, would form a capacitance of C ; a short HV line from the HV network to the last electrode would yield an inductance of L ; also, individual anodes are terminated with a resistance of R . This RLC loop could prevent a fast voltage recovery of the last electrode. It's very easy to have the underdamped response which leads to a decaying sine (ringing). Therefore, the electrode voltage variation simultaneously induces the same crosstalk on all anodes, since the second MCP layer is the same as all anode channels [8].

Discussion and conclusion

In summary, the measured performance of each channel is listed in Table 1. With typically $TTS < 60$ ps and stable gain $> 10^7$, the MCP-PMT shows excellent timing performance and the potential of achieving better spatial resolution by further pixelation.

To further improve the performance of MCP-PMT, there are two possible ways to minimize the distortion of waveforms. One is to disconnect this RLC loop circuit by making a segmentation of the last MCP electrode facing four anodes and set up four separate HV networks. The other is to use a damping resistance to match the inductance and the capaci-

Fig. 10 Anode signals A1–A4 with 20 mv/div in vertical and 10 ns/div in horizontal. A1 is induced by a single photon through a 1 mm diameter aperture and the others are crosstalk

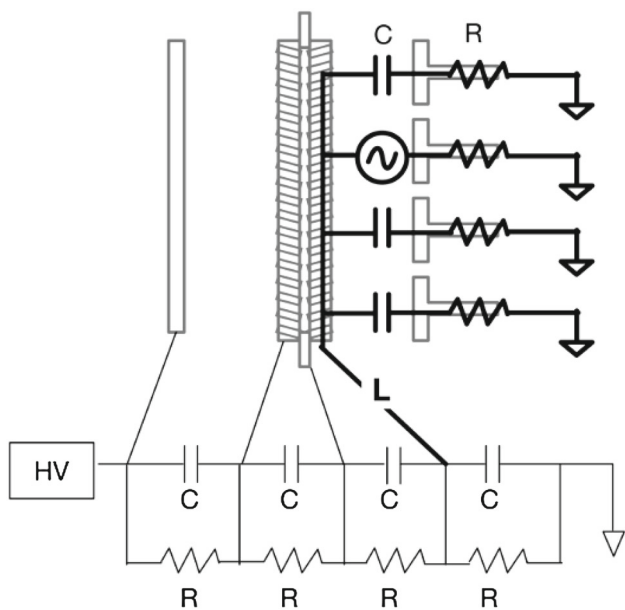
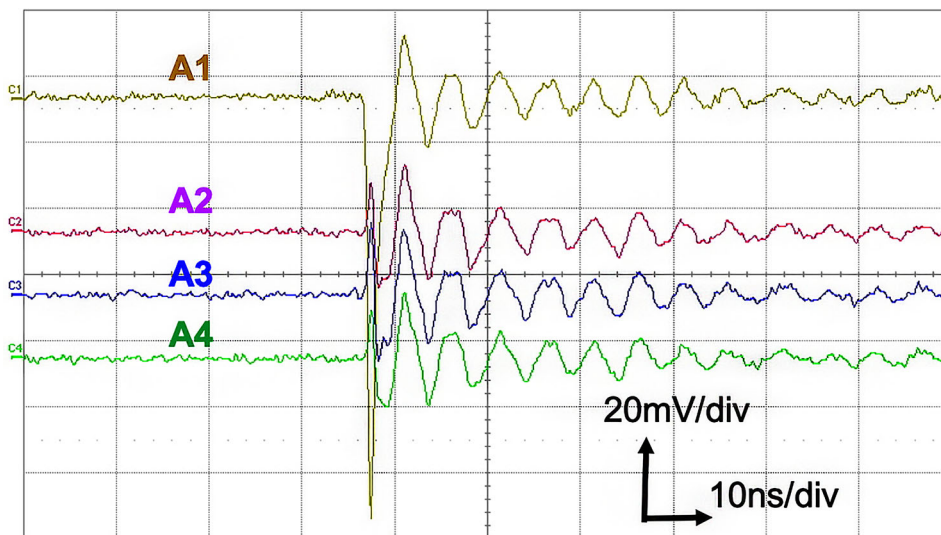


Fig. 11 Schematic drawing of an electric equivalent circuit [8]

Funding This research work is supported by the National Natural Science Foundation of China, Nos. 11775217 and 11675172.

References

1. M. Aleksa, et al., Strategic R&D, Programme on Technologies for Future Experiments No. CERN-OPEN-2018-006 (2018)
2. L. Linssen, Technological challenges of future HEP experiments, *Presentation, Open Symposium*, Canada, Spain (2019)
3. The CMS Collaboration, *Technical Proposal for the Phase-II of the CMS*, CERN-LHC-2015-010/LHCC-p-008. <https://cds.cern.ch/record/2020886>
4. H.F.-W. Sadrozinski, A. Seiden, N. Cartiglia, 4D tracking with ultra-fast silicon detectors. *Rep. Prog. Phys.* **81**, 026101 (2018)
5. A. Bornheim et al., LYSO based precision timing calorimeters. *J. Phys: Conf. Ser.* **928**, 012023 (2017)
6. A. Papanestis, Cherenkov light imaging in particle and nuclear physics experiments. *NIM A* **952**, 162004 (2020)
7. M. Shayduk et al., Light sensors selection for the Cherenkov telescope array: PMT and SiPM. *NIM A* **695**, 109–112 (2012)
8. K. Inami et al., Cross-talk suppressed multi-anode MCP-PMT. *Nucl. Instrum. Methods Phys. Res. Sect. Accel. Spectrom. Detect. Assoc. Equip.* **592**(3), 247–253 (2008)

Table 1 Measured characteristics of the MCP-PMT

Channel	Gain	TTS (ps)	Rise time (ps)
A1	1.29e7	53	357
A2	1.25e7	56	352
A3	1.25e7	54	358
A4	1.28e7	54	362

tance. Whether these methods will work remains to be further studied.